



ISSN: 0067-2904

Effect of Temperature on the Working Parameters of Negative Corona Discharge with Coaxial Electrodes Configuration

Mustafa K. Jassim¹, Enas A. Jawad*¹, Jamal K. Alsaide²

¹Department of Physics, College of Education for Pure Science (Ibn Al – Haitham), University of Baghdad

²Ministry of Science and Technology, Baghdad, Iraq

Abstract

The influence of ambient temperature on the various parameters of negative corona discharge in atmospheric dry air with coaxial cylindrical electrodes is investigated. The calculations are achieved using the finite element method by COMSOL Multiphysics software. The investigation aims to notice the effect many of working temperatures on the I-V characteristic curve of negative corona discharge in the air. The calculations of several parameters (electron density, temperature, ...) are presented visually and discussed. The results of the work are compared with theoretical and experimental data and they are in a good agreement.

Keywords: Negative Corona Discharge, I-V curve characteristic, COMSOL Multiphysics

تأثير درجة الحرارة على معاملات العاملة بتفريغ الهالة ذا نظام اقطاب متحدة المحور

مصطفى كامل جاسم¹، إيناس جواد أحمد*¹، جمال كاظم الساعدي²

¹قسم الفيزياء، كلية التربية للعلوم الصرفة (ابن الهيثم)، جامعة بغداد

²وزارة العلوم والتكنولوجيا، بغداد، العراق

الخلاصة

تم دراسة تأثير درجة الحرارة المؤثرة على مختلف معاملات تفريغ الكورونا (الأكليل - الهالة) تحت الهواء الجوي ذا الأقطاب الكهربائية المحورية. أنجزت الحساب باستخدام طريقة العناصر المحدودة بواسطة برنامج كومسول متعدد الفيزياء. يهدف البحث التحقق من تأثير درجات حرارة العمل على منحنى I-V المميز لتفريغ الكورونا السالب في الهواء. تم تقديم الحسابات عدة معاملات مؤثرة بشكل رسوم ومناقشتها. أخيراً تم مقارنة نتائج العمل مع البيانات النظرية والتجريبية وهم في اتفاق جيد جداً.

Introduction

The corona discharge is one of the types of electrical discharge, characterized by a corona lighting creation and set up from the gas ionization around the surface of conductor [1]. The discharge has normally taken place in high-voltage systems when the electrical field strength surrounded by the electrode is high enough but is not high for electrical breakdown between nearby connectors to happen [2]. If the electrical field is high enough, the gas surrounding it at that point comes in and becomes conductive, and the electric field intensity at this point becomes very higher. As a consequence, it makes for the electron to drift and ionize of the gas around the cathode and spread out towards the anode [3]. More electrons will generate through secondary emission at the cathode by the positive ions. The secondary electrons are accountable for sustaining the corona discharge. The ambient gas becomes partially conductive, increasing the conductive area. The current flows from the high voltage

*Email: dr_enasahmedja@yahoo.com

electrode (cathode) to the surrounding gas and ionized it, producing a plasma around the electrode [4]. The generated ions will flow to the nearby low-voltage electrode (anode). Thus, the ionization occurs near the cathode and the charges slowly find their way to move to the low voltage electrode in order to be electrically neutralized [5]. The discharge emits light with colour is often blue in the air near the conductive metal attached to the high voltages.

There are three types of corona discharge; positive, negative and self-repetitive. The positive corona is established when the electrode is connected to the positive end of the power supply while the negative corona is build-up when the electrode is connected to the negative terminal. The self-repetitive corona is established in both cases of the negative and positive case [6]. The last case takes place at relatively low voltage when the discharge stopping itself because of the build-up of the space charge at near the sharp electrode and disappears by the diffusion and then recombine. In practice, corona discharge is used to clean the air by ionization, to neutralized contaminants and to kill microbes. Merely in the transmission lines, it causes power loss, damages the conductors and insulators and causing radio frequency noise that interferes with communication signals [7].

This study is done on the DC negative corona, which two coaxial electrodes in air under atmospheric pressure for steady-state regimes. This type of discharge is easy and has many environmental applications [8]. We suppose wire- in-cylinder geometries. The inner electrode is the cathode and the outer is the grounded anode. The radius of the cathode is (100 μm) and separated from the anode by a 10 cm gap. The anode is grounded and the cathode has 10s kV applied to sustain the discharge. The used model describes the charge particle behavior by utilizing fluid equations and it is supposed that the discharge is uniform and diffuse in the radial direction.

In this study, we use COMSOL Multiphysics for the proposed investigation. The program is a finite element method software for many engineering and physics applications allowing to introduce couples of ordinary and partial differential equation systems [9]. The objective of this work is to testify how the charged particles created in the corona discharge, how it transport, and obtain the I-V curves at different ambient temperatures at constant air number density.

Theory and model

The following set of equations is used to compute the ionization of the neutral gas. Further, to compute the flux of charged particles as the negative electric potential is applied at the cathode. The electron and ions continuity and momentum equations are solved simultaneously in the program. These equations with the drift-diffusion approximation with Poisson's equation are self-consistently coupled.

The electron density is computed by solving the diffusion-drift equation [10]

$$\frac{\partial}{\partial t}(n_e) + \nabla \cdot \{-n_e(\boldsymbol{\mu}_e \cdot \mathbf{E}) - \mathbf{D}_e \cdot \nabla n_e\} = R_e \quad (1)$$

where the source coefficients R_e is determined by the plasma chemistry by using the rate coefficients and given by [10]

$$R_e = \sum_{j=1}^M k_j x_j N_n n_e \quad (2)$$

where j is the reaction, k_j is the rate coefficient, x_j is the mole fraction of the target, and N_n is the total neutral number density.

Utilizing local field approximation, the equation, which relates the reduced electric field E/N and electron energy ε

$$\varepsilon = F(E/N) \quad (3)$$

Electron diffusivity (\mathbf{D}_e) is calculated from the mobility of electron ($\boldsymbol{\mu}_e$) using the equation

$$\mathbf{D}_e = \boldsymbol{\mu}_e T_e \quad (4)$$

The following equation is solved for the mass fraction of heavy ions

$$\rho \frac{\partial y}{\partial x}(w_k) + \rho(\mathbf{u} \cdot \nabla)w_k = \nabla \cdot \mathbf{j}_k + R_k \quad (5)$$

The electrostatic field is calculated using the following equation [11]

$$-\nabla \cdot \varepsilon_0 \varepsilon_r \nabla V = \rho \quad (6)$$

where the space charge density ρ calculated depending on the plasma chemistry defined in the model utilizing the formula [12]

$$\rho = q[\sum_{k=1}^N Z_k n_k - n_e] \quad (7)$$

There are boundary conditions for the electron flux due to the electrons that lost to the wall because of the random motion and gained because of the secondary emission effects

$$\mathbf{n} \cdot \Gamma_e = \frac{1}{2} v_{e,th} n_e - \sum_p \gamma_p (\Gamma_e \cdot \mathbf{n}) \tag{8}$$

where γ_p is the secondary emission coefficient. Respect to the heavy ions, they are lost to the wall because of the surface reactions and the electric field is pointed to the wall

$$\mathbf{n} \cdot \mathbf{j}_k = M_w R_k + M_w c_k Z \mu_k (\mathbf{E} \cdot \mathbf{n}) \{ Z_k \mu_k (\mathbf{E} \cdot \mathbf{n}) > 0 \} \tag{9}$$

To simplify the numerical simulation, a step function is used to modulate V_0 with the transient potential supposing that

$$V = V_0 \tanh(t/\tau) \tag{10}$$

Further, the model utilizes a Scharfetter-Gummel upwind scheme to eliminate the numerical instabilities in the charged particle number density coupled with the finite element method.

Chemistry of plasma in air

Despite the chemistry of plasma in the air are very complex due to the hundreds of reactions involved for the main excited states, we use a simplified group of reactions. This group denotes the correct reactions in the dry air. It is assumed that the air consists of 20% oxygen and 80% nitrogen. Furthermore, we assumed that a general species of type A is used for the air. The species A may be ionized to form positive ions and may attach electrons to form negative ions. The creation and destruction of electrons are described by ionization, attachment Townsend coefficients, three body attachment, and recombination of electron-ion in the whole volume.

By using the set of electron cross sections of Oxygen and Nitrogen in Boltzmann solver of the program the Townsend coefficients are getting as a function of the mean electron energy. Table-1 shows the considered reactions in the model. In addition to these reactions, there are reactions related to the surface; $p \rightarrow A$ and $n \rightarrow A$ with sticking coefficients of 1. The ions reach the walls change to be neutral atoms.

Table 1-Table of chemical reactions involved.

$e + A \rightarrow p + 2e$	Ionization
$e + A \rightarrow n$	Attachment
$e + 2A \rightarrow n + A$	Attachment
$e + p \rightarrow A$	Reaction
$n + p \rightarrow 2A$	Reaction

Results and discussion

Figure-1 illustrates the variation of electron density with the radial position of the electrical discharge model at different temperatures and constant background gas density. The calculations introduced here are corresponding to a steady state operation. This means that the ions are the main species in the plasma and imposed that equal density of both negative and positive ions and a small density portion of electrons. The density of electrons increases as they accelerated from the cathode through a small region where they have enough energy to reach the peak and then decrease to the saturation state at the anode region. The ionization here creates new electron-ion pairs. Obviously, the greater the temperature, are the higher the upward trending towards increasing the density of electrons. The curves were drawn by the logarithmic scale of the r-coordinate in order to illustrate the difference between the different temperature curves, otherwise, the curves would overlap on each other in small domain. It should be noted that the corona discharge in air requires very high voltage to reach the breakdown.

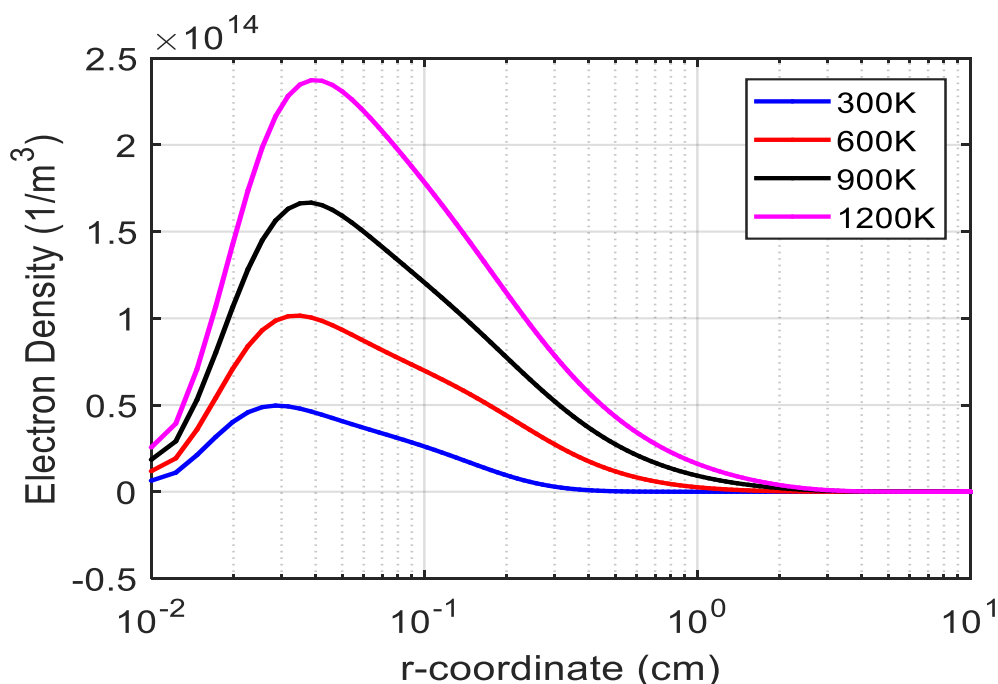


Figure 1-The electron density against radial position of electric discharge for various temperatures.

Figure-2 shows the distribution of positive ion density along the radius of the electrical discharge model at different temperatures. Positive ion density is at the top of its value at the cathode and then starts decreasing to zero at the anode. As the temperature is increased there will be a higher upward trend towards the increasing the density of positive ions. At lower temperatures, it reaches to the zeroth value before the highest temperature as we turn towards the anode to sustain the discharge. The reason for that is that the oxygen is electronegative and the value of electron collision frequency is high due to vibrational and rotational interactions. Furthermore, in the region near the cathode, most of the ionization takes place, while the rest volume of discharge reaches to the anode.

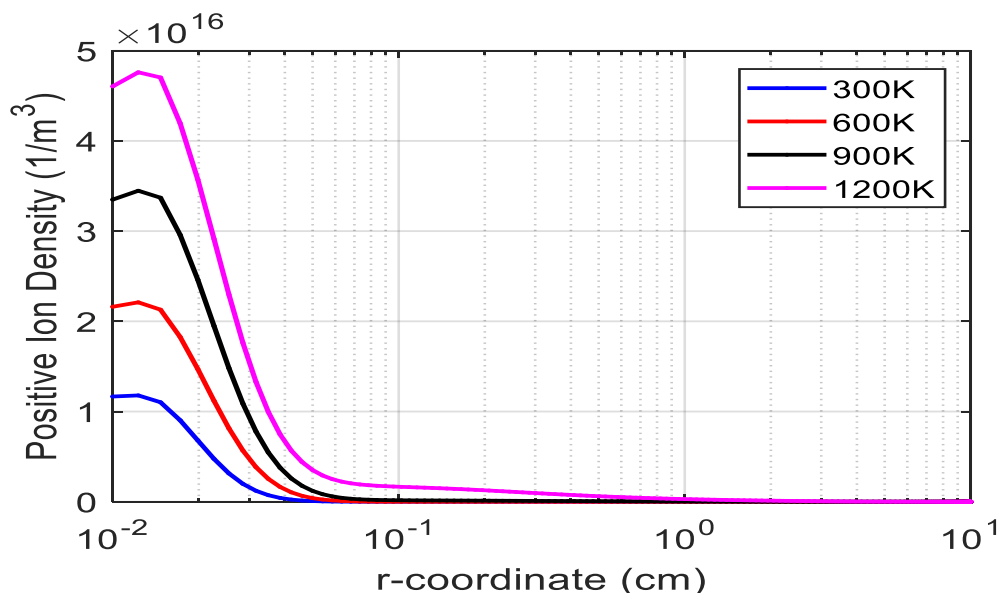


Figure 2- The positive ion density against radial position of electric discharge for various temperatures.

Figure-3 presents the spread of negative ions along the radius between the cathode and the anode of the discharge. The Gaussian distribution of the curve is observed along the radius. The peak of the curve at 300 K temperature is higher than the rest of the curves and is a shift towards the anode, and as

the temperature increases, the shift of the curve rises towards the cathode with higher peak. At the region near the cathode, the temperature effect rises in the curve as the temperature increases.

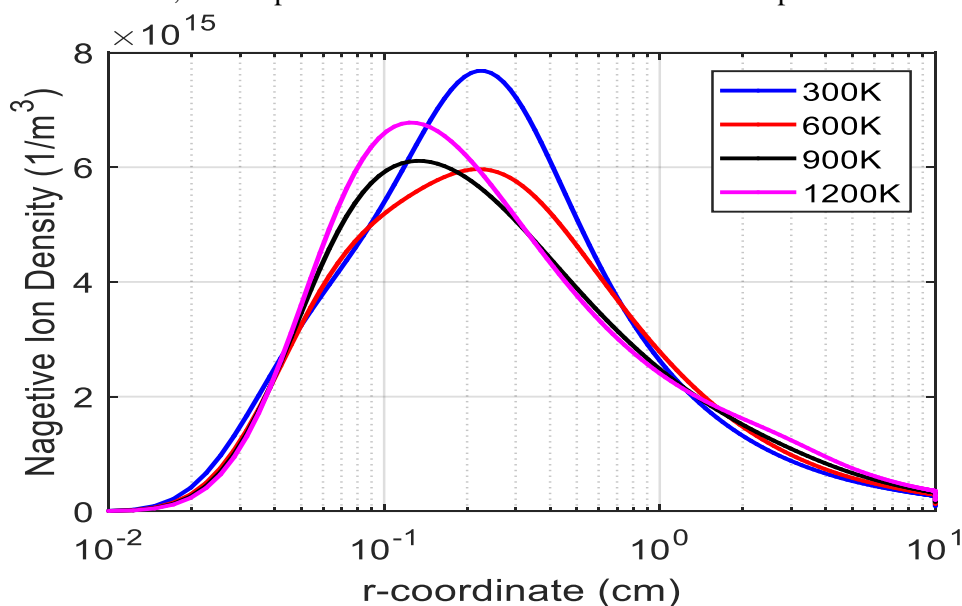


Figure 3-Negative ions density against radial position of electric discharge for various temperatures.

Figure-4 shows the spatial distribution of the electron temperature along the distance between the cathode and the anode at different temperatures. In general, the curves have the same attitude with different behaviour in the vicinity of the anode where the temperature effect is shown by the temperature of the electron at the lower temperatures. It is noted that the middle area between the anode and cathode is very close to the electron temperature. In the vicinity of the cathode, the temperature of the electron increases with increases of temperature, while in the nearby region of the anode the electrons do not ionize because they have not enough energy. Consequently, the ions drifting to the anode dominated the spatial part of the discharge.

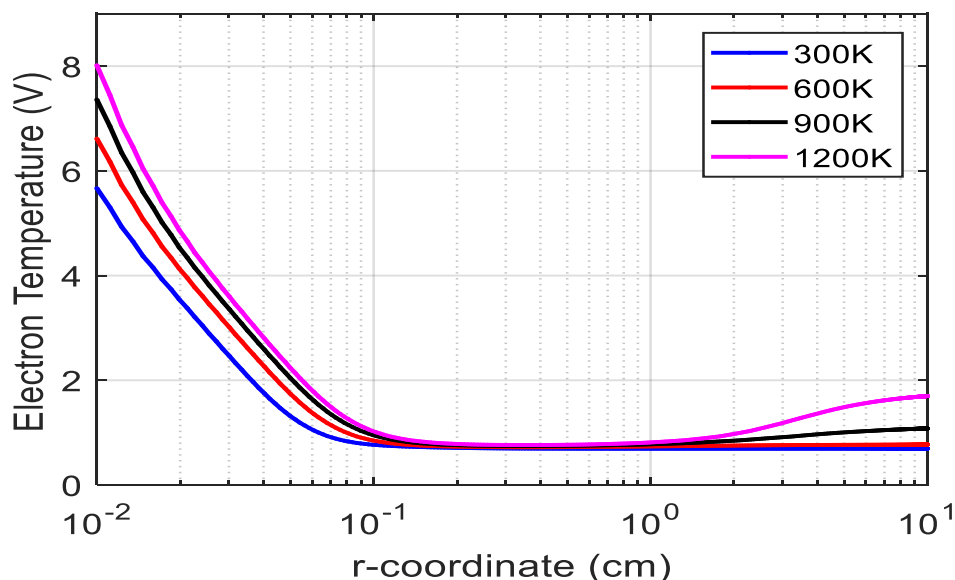


Figure 4-Electron temperature against radial position of electric discharge for various temperatures

Figure-5 shows the electric potential variation along the radial distance between the cathode and the anode at different temperatures. It is clear that the curves for whole used temperatures have the same potential in the region near the cathode area. The electric potential exponentially increases to the top to be at a similar value at the anode region. In the area between the cathode and the anode, the

curve is more concave at the larger temperatures. Further, the charge separation hardly distorts the applied electric potential at nearby the anode.

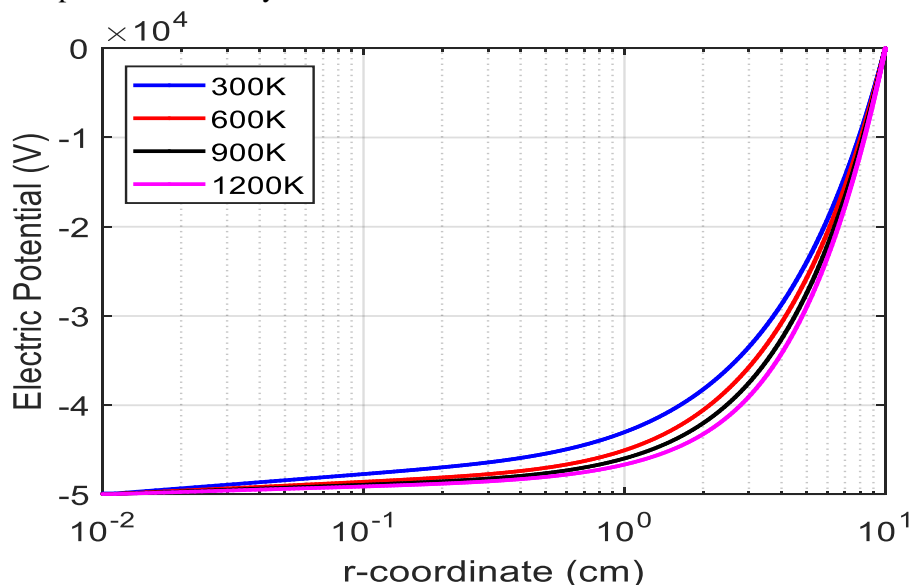


Figure 5-The electric potential against radial position of electric discharge for various temperatures.

Figure-6 illustrates the changes in the reduced electric field along the distance between the cathode and the anode at various temperatures. This behaviour is similar to the electron temperature in the Figure-2b. However, the temperature effect is clearly visible in the region near the anode due to the rise of the curve as the temperature increases.

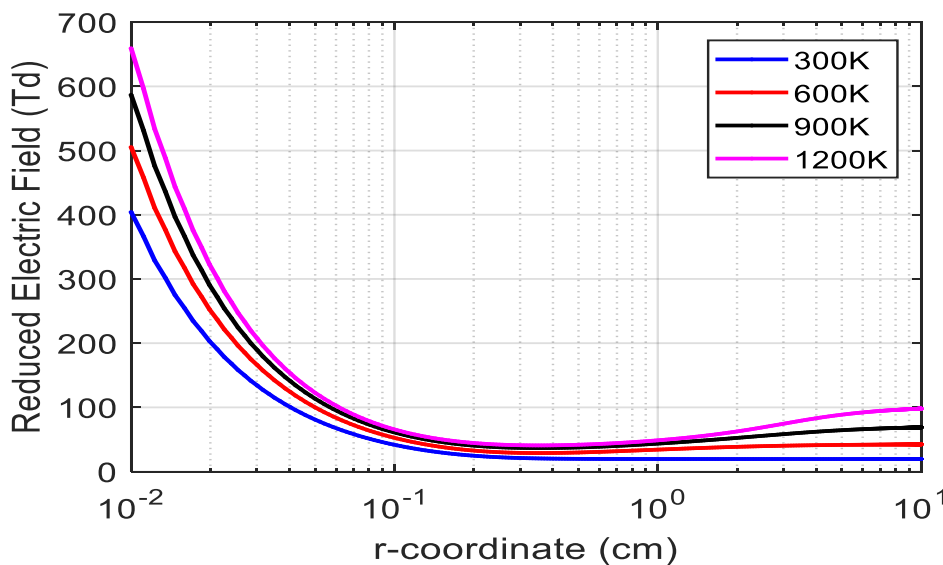


Figure 6-The reduced electric field against radial position of electric discharge for various temperatures.

Figure-7 shows the I-V characteristics of the discharge at various temperatures. Clearly, the total ion current is increased with the increased applied voltage. As the ambient temperature increases the total ion current density increased at each point along the distance between the cathode and the anode. The figure expresses that the total ion current density at the same applied voltage increased. The whole curves are following a quadratic law. Further, since the charge particles density and mobility of ions are low, the discharge has a high resistivity. The results obtained in this work are in a good agreement with theoretical and experimental literature [7, 13].

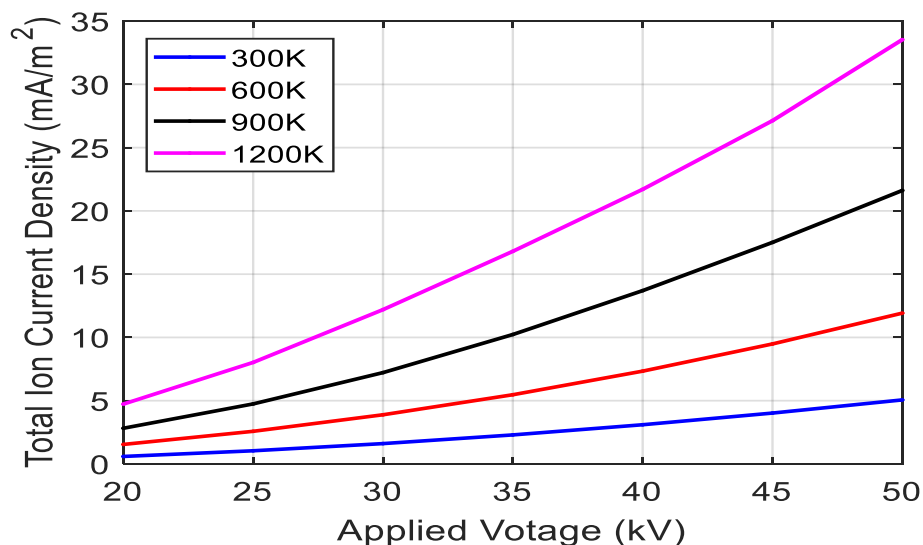


Figure 7-The total ion current density against applied voltage of electric discharge for various temperatures.

Figure-8 shows the distribution of electron density in the volume of discharge at different temperatures. The cathode with strongly negative potential repels electrons and accelerates positive ions towards it. As a result, there is an ion separation region where strong electric field and the negative electrons are accelerated to higher energy then capable of ionizing the gas. The ionization region around the cathode enlarged as the temperature increased.

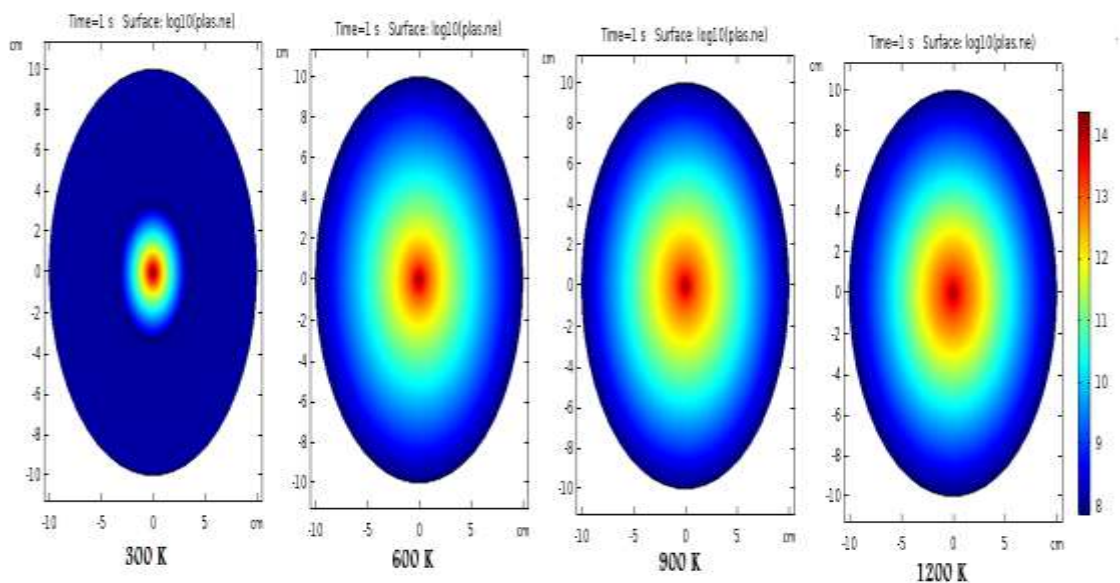


Figure 8-The distribution of electron density in the volume of discharge for electric discharge for various temperatures.

Conclusion

Negative corona discharge in atmospheric air is investigated in this paper. The work calculates the I-V characteristics of the system at various temperatures and at atmospheric air. The I-V diagram indicates that the curve is raised as the temperature increased. The electron temperature and reduce electric field are decreasing as the radial distance from cathode to anode increased. The effect of temperature is clearly shown at the nearby region of anode by raising the curve tail as the temperature increased. In addition, the applied potential at the coaxial wires is determined along the radial distance

from cathode to anode. Here, the effect of temperature shows the concave increasing up of the curve by increasing the temperature. Finally, the simulation work shows the distribution of electron density in the bulk of discharge at different temperatures.

References

1. Yu D. **2007**. Study of electric discharge and space charge formation phenomena in the air gaps of an ice-covered insulator using an icicle/ice-covered plate electrode system, PhD. Thesis, University of Québec, Canada.
2. Holboell J. and Sverrisson S. **2015**. The influence of temperature differences in moist environments on surface discharges on solid insulation, 24th Nordic Insulation Symposium on Materials, Components and Diagnostics. Technical University of Denmark, Copenhagen, Denmark 134-137.
3. Arora R. and Mosch W. **2011**. *High Voltage and Electrical Insulation Engineering*. Wiley, Hoboken, NJ, USA.
4. Sigmond R. **1997**. The Oscillations of the Positive Glow Corona. *Journal de Physique IV Colloque*, **07(C4)**: 383-395.
5. Shang J. J. **2018**. Modelling Plasma via Electron Impact Ionization, *Aerospace*, **5** (2): 1-25.
6. Goldman M., Goldman A. and Sigmond R. S. **1985**, The corona discharge, its properties and specific uses, *Pure & Appl. Chem.*, **57(9)**: 1353-1362.
7. Panicker P. K. **2003**. *Ionization of air by corona discharge*, MSc thesis, University of Texas, USA.
8. Veldhuizen E.M. **1999**. *Electrical Discharges for Environmental Purposes: Fundamentals and Applications*, Nova Science Publishers, New York, ISBN 1-56072-743-8.
9. Umeozor C. J. **2013**. Computer simulation of the methane plasma enhanced deposition of carbon film. MSc thesis, University of Missouri, USA.
10. Plasma Module User's Guide. **2017**. Theory for the Drift Diffusion Interface. Version: COMSOL 5.3
11. Plasma Module User's Guide. **2017**. Theory for the Heavy Species Transport Interface. Version: COMSOL 5.3
12. Plasma Module User's Guide. **2017**. Theory for the Electrostatics Interface Version: COMSOL 5.3
13. Fulyful F. K. **2008**. High Temperature-High Pressure Effect on Performance of an Electrostatic precipitator, *Journal of Karbala University*, **6(2)** Scientific: 84-92